American Journal of Engineering Research (AJER)
e-ISSN: 2320-0847 p-ISSN : 2320-0936
Volume-4, Issue-7, pp-01-09
www.ajer.org
Research Paper Open Access

Numerical solution of MHD flow in presence of induced Magnetic field and hall current Effect Over an Infinite Rotating vertical Porous plate through porous medium

P. Biswas[1], A. Biswas[2], M. K. Das[3] & S. F. Ahmmed[4]
[1,2,3,4] *Mathematics Discipline, Khulna University, Khulna-9208*
pronabbiswas16@gmail.com[1], abku07@gmail.com [2], mahadeb.ku@gmail.com [3] and sfahmmed@yahoo.com[4]

ABSTRACT: *The one dimensional MHD unsteady magneto-hydrodynamics fluid flow past an infinite rotating vertical porous plate through porous medium with heat transfer considering hall current has been investigated numerically under the action of induced magnetic field. The numerical solution for the primary velocity field, secondary velocity field and temperature distributions are obtained by using the implicit finite difference method. The obtained results have been represented graphically for different values of parameters. Finally, the important findings of the investigation are concluded.*

Keywords: *MHD, rotating porous plate, porous medium, heat transfer, hall current, finite difference method.*

I. INTRODUCTION

In astrophysical and geophysical studies, the MHD boundary layer flows of an electrically conducting fluid have also vast applications. Many researchers studied the laminar flow past a vertical porous plate for the application in the branch of science and technology such as in the field of mechanical engineering, plasma studies, petroleum industries Magneto hydrodynamics power generator cooling of clear reactors, boundary layer control in aerodynamics and chemical engineering. Many authors have studied the effects of magnetic field on mixed, natural and force convection heat and mass transfer problems which have many modern applications like missile technology used in army, nuclear power plant, parts of aircraft and ceramic tiles. Indeed, MHD laminar boundary layer behavior over a stretching surface is a significant type of flow having considerable practical applications in chemical engineering, electrochemistry and polymer processing. This problem has also an important bearing on metallurgy where magneto hydrodynamic (MHD) techniques have recently been used.

H. L. Agarwal and P. C. Ram [1] have studied the effects of Hall Current on the hydro-magnetic free convection with mass transfer in a rotating fluid. H. S. Takhar and P. C. Ram [2] have studied the effects of Hall current on hydro-magnetic free convective flow through a porous medium. B. K. Sharma and A. K. Jha [3] have analyzed analytically the steady combined heat and mass transfer flow with induced magnetic field. B. P. Garg [4] has studied combined effects of thermal radiations and hall current on moving vertical porous plate in a rotating system with variable temperature. Dufour and Soret Effects on Steady MHD Free Convection and Mass Transfer Fluid Flow through a Porous Medium in A Rotating System have been investigated by Nazmul Islam and M. M. Alam [5]. Hall Current Effects on Magneto hydrodynamics Fluid over an Infinite Rotating Vertical Porous Plate Embedded in Unsteady Laminar Flow have been studied by Anika et al [6]. S. F. Ahmmed and M. K. Das [7] have investigated Analytical Study on Unsteady MHD Free Convection and Mass Transfer Flow Past a Vertical Porous Plate.

Abo-Eldahab and Elbarbary [8] have studied the Hall current effects on MHD free-convection flow past a semi-infinite vertical plate with mass transfer. The effect of Hall current on the steady magneto hydrodynamics flow of an electrically conducting, incompressible Burger's fluid between two parallel electrically insulating infinite planes have been studied by M. A. Rana and A. M. Siddiqui [9].

Hence our aim is of this paper is to extend the work of Anika.et al. [6] to solve the problem by implicit finite difference method. The proposed model has been transformed into non-similar coupled partial differential equation by usual transformations. Finally the comparison results have been shown graphically as well as tabular form.

II. MATHEMATICAL MODEL OF THE FLOW

Let us consider an unsteady electrically conducting viscous incompressible, laminar fluid flow through a vertical porous plate. The fluid is assumed to be in the x-direction which is taken along the porous plate in upward direction and y-axis is normal to it. Let the unsteady fluid flow starts at t=0 afterward the whole frame is allowed to rotate about y-axis with t>0,the plate started to move in its own plate with constant velocity U and temperature of the plate is raised to T_w to T_∞ A strong uniform magnetic field B_o is applied normal to the plate that induced another magnetic field on electrically conducting fluid. In the presence of magnetic field. Then the fluid is affected by hall current, which gives rise t a force in z-direction. The physical configuration of the problem is furnished in Figure- a. Thus according to above assumptions the governing boundary layer equations with Bounssineq's approximation are:

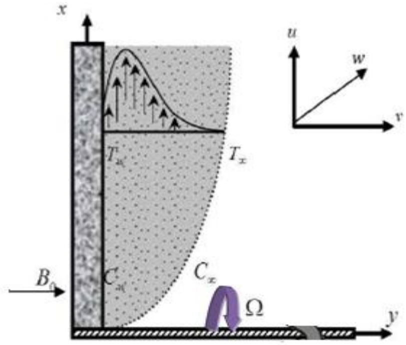

Figure- a. Physical configuration and co-rdinate system

$$\frac{\partial u}{\partial t} - v_0 \frac{\partial u}{\partial y} = \upsilon \left(\frac{\partial^2 u}{\partial y^2} \right) + g\beta (T - T_\infty) - \frac{\sigma' B_0^2}{\rho(1+m^2)}(u + mw) + 2Rw - \frac{\mu}{\rho k} u \quad (1)$$

$$\frac{\partial w}{\partial t} - v_0 \frac{\partial w}{\partial y} = \upsilon \left(\frac{\partial^2 w}{\partial y^2} \right) - \frac{\sigma' B_0^2}{\rho(1+m^2)}(mu - w) - 2Ru \quad (2)$$

$$\frac{\partial T}{\partial t} - v_0 \frac{\partial T}{\partial y} = \left(\frac{K}{\rho c_p} \frac{\partial^2 T}{\partial y^2} \right) + \frac{1}{c_p} \upsilon [(\frac{\partial u}{\partial y})^2 + (\frac{\partial w}{\partial y})^2] \quad (3)$$

With corresponding boundary conditions

$$t > 0; \begin{cases} u = U_0, w = 0, T = T_w \quad at\ y = 0 \\ u = 0, w = 0, T \to T_\infty \quad as\ y = \infty \end{cases} \quad (4)$$

where u, v and w are the x, y and z components of velocity vector, m_e is the Hall parameter, where e is the electron frequency, is the kinematic coefficient viscosity, is the fluid viscosity, is the density of the fluid, is the thermal conductivity, C_p is the specific heat at the constant pressure, K is the thermal diffusion ratio, respectively. The rotation is described by the R .

III. MATHEMATICAL FORMULATION

To obtain the governing equations and the boundary condition in dimension-less form, the following non-dimensional quantities are introduced as;

$$Y = y\frac{U_0}{u}, U = \frac{u}{U_0}, W = \frac{w}{U_0}, \tau = t\frac{U_0^2}{\upsilon}, \overline{T} = \frac{T - T_\infty}{T_w - T_\infty}$$

Using the above non-dimensional parameters, we get the governing equation with boundary conditions in the following form,

$$\frac{\partial U}{\partial \tau} - S\frac{\partial U}{\partial Y} = \frac{\partial^2 U}{\partial Y^2} + G_r T - \frac{M}{(1+m^2)}(u + mw) + 2RW - KU \quad (5)$$

$$\frac{\partial W}{\partial \tau} - S\frac{\partial W}{\partial Y} = \frac{\partial^2 W}{\partial Y^2} + \frac{M}{(1+m^2)}(u + mw) - 2RU \quad (6)$$

$$\frac{\partial T}{\partial t} - S\frac{\partial T}{\partial y} = \frac{1}{P_r}\frac{\partial^2 T}{\partial Y^2} + E_c[(\frac{\partial U}{\partial Y})^2 + (\frac{\partial W}{\partial Y})^2] \quad (7)$$

With corresponding boundary conditions

$$t > 0; \begin{cases} U = 1, W = 0, T = 1 \;\; at\, Y = 0 \\ U = 0, W = 0, T = 0 \;\; as\, Y = \infty \end{cases} \tag{8}$$

Where t represents the dimensionless time, Y is the dimensionless Cartesian coordinate, U and W are the dimensionless velocity component in X and Z direction, T is the dimensionless temperature

$S = \frac{\upsilon_0}{U_0}$ (Suction parameter), $G_r = \frac{g B_T (T_w - T_\infty)\upsilon}{U^3_0}$ (Grashoff Number), $M = \frac{\sigma B^2_0 \upsilon}{\rho U^2_0}$ (Magnetic parameter), $P_r = \frac{\rho C_p \upsilon}{\mathrm{K}}$ (Prandlt Number), $R = \frac{L\upsilon}{U^2_0}$ (Rotation parameter), $m = \frac{\sigma_e B_0}{en}$ (hall parameter), $E_c = \frac{U^2_0}{C_p (T_w - T_\infty)}$ (Eckert Number)

IV. NUMERICAL SOLUTIONS

In order to solve the non-dimensional system by the implicit finite difference technique, it is required a set of finite difference equations. In this case, the region within the boundary layer is divided by some perpendicular lines of Y -axis, where Y -axis is normal to the medium as shown in Figure- b. It is assumed that the maximum length of boundary layer is $Y_{max} = 25$ as corresponds to Y i.e. Y varies from 0 to 25 and the number of grid spacing in Y-directions is $P = 400$, hence the constant mesh size along Y axis becomes $\Delta Y = 0.0625 (0 \le Y \le 25)$ with a smaller time-step $\Delta t = 0.001$ Let U', W' and C' denotes the values of U, W and C at the end of time-step respectively.

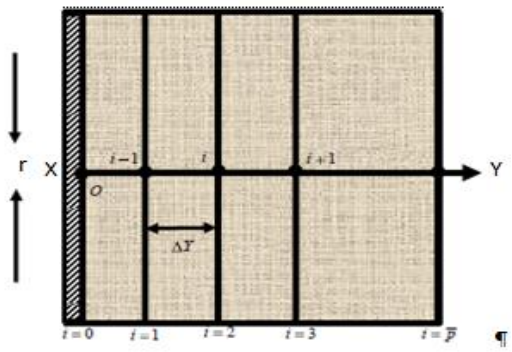

Figure-(b): Implicit finite differece space grid

Using the implicit finite difference approximation, the following appropriate set of finite difference equations are obtained as;

$$\frac{U^{n+1}_i - U^n_i}{\Delta\tau} - S\frac{U^n_{i+1} - U^n_i}{\Delta Y} = \frac{U^n_{i+1} - 2U^n_i + U^n_{i-1}}{(\Delta Y)^2} + G_r \overline{T} - \frac{M}{(1+m^2)}(U^n_i + mW^n_i) \tag{9}$$

$$+2RW^n_i - KU^n_i$$

$$\frac{W^{n+1}_i - W^n_i}{\Delta\tau} - S\frac{W^n_{i+1} - W^n_i}{\Delta Y} = \frac{W^n_{i+1} - 2W^n_i + W^n_{i-1}}{(\Delta Y)^2} + \frac{M}{(1+m^2)}(mU^n_i - W^n_i) - 2RU^n_i \tag{10}$$

$$\frac{T^{n+1}_i - T^n_i}{\Delta\tau} - S\frac{T^n_{i+1} - T^n_i}{\Delta Y} = \frac{1}{P_r}\frac{T^n_{i+1} - 2T^n_i + T^n_{i-1}}{(\Delta Y)^2} + E_c\left[\left(\frac{U^n_{i+1} + -U^n_i}{\Delta Y}\right)^2 - \left(\frac{W^n_{i+1} + -W^n_i}{\Delta Y}\right)^2\right] \tag{11}$$

with the finite difference boundary conditions,

$$U^n_{0,j} = 0; V^n_{0,j} = 0; \overline{T}^n_{0,j} = 0$$

$$t > 0; \begin{cases} U^n_{i,0} = 1; W^n_{i,0} = 0; \overline{T}^n_{i,0} = 1 \\ U^n_{i,L} = 0; V^n_{i,L} = 0; \overline{T}^n_{i,L} = 0 \end{cases} \tag{12}$$

Here the subscript i designates the grid points with Y coordinate and the superscript n represents a value of time, $t = n\Delta t$, where $n = 0, 1, 2 \ldots\ldots\ldots$. The primary velocity U secondary velocity W, temperature T distributions at all interior nodal points may be computed by successive applications of the above finite difference equations. The numerical values of the shear stresses, Nusselt number are evaluated by Five-point approximate formula.

V. RESULTS AND DISCUSSION

For observing the physical situation of the unsteady state situations have been illustrated in Figure–1 to Figure-27 up to dimensionless time t=80.00, but at the present case the changes appear till t=60.Therefore t=60 represents the steady state solution of the problem. The primary velocity, secondary velocity and temperature distributions are displayed for various values of m, M, G_r, P_r, R, S in Figure–1 to Figure-18 to the time step t= 1,10,60 and Share stress and Nusselt Number are shown in Figure-19 to Figure-27 at the same time step. These results shows that the primary velocity and secondary velocity are increase with the increase of R, G_r, and E_c, and decrease with the increase of M, P_r, S so it follows the boundary conditions both for primary and secondary velocities. It is noted that the temperature distribution is increased with the increase of G_r and decrease with the increase of M, P_r, and S. The velocities are shown in Figure -1 to Figure -14.for different values of the parameter m, M, G_r, P_r, S. $P_r=0.71$ has been used for air at 20^0C, $P_r=1.00$ has been used for electrically solution like saline water at 20^0C, $P_r=7.00$ has been used to water at 20^0C. The other parameters are used arbitrarily. The effect of P_r causes fall of temperature at the same values of Prandlt number P_r. Therefore Heat is able to diffuse away more rapidly and for large suction S. The velocity profile decrease drastically where as the secondary velocity decrease severally with the increase of S. This is because sucking decelerates fluid particles through the wall reducing the growth of the boundary layer as well as thermal boundary layer, Shown in Figure -13 to Figure -14. The share stress t_x increase for the values of $G_r \geq 1$. The Nusselt Number *(-Nu)* has increased with the increase of P_r and S in Figure -25 and Figure -27. The dimensionless Parameter R, G_r, and E_c resists the time development of Nusselt-Number(-Nu) in X-direction shown in Figure -23, Figure -24 and figure-26.respectively The share stress t_x is increased with the increase of R, G_r and E_c, shown in Figure -19, Figure -(20) and Figure -22 .The suction parameter S caused effects for different values on share-stress. The share-stress falls drastically for large suction and *(-Nu)* rises severally with the increase of suction S, shown in Figure -21 and in Figure -27 respectively.

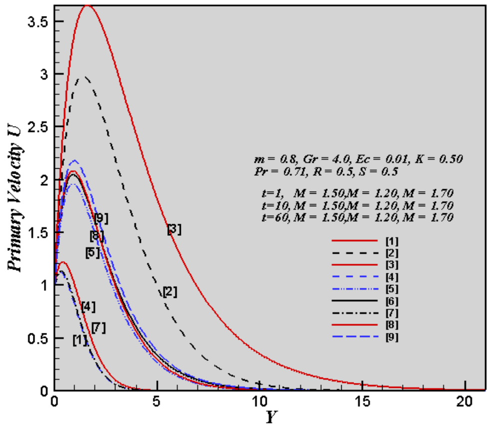

Figure- 1. Primary velocity profiles for the parameter *M*

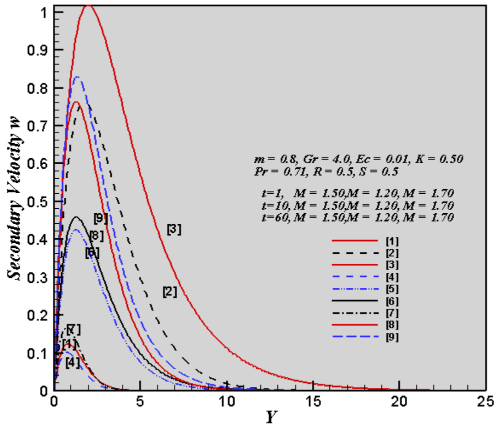

Figure- 2. Secondary velocity profiles for the parameter *M*

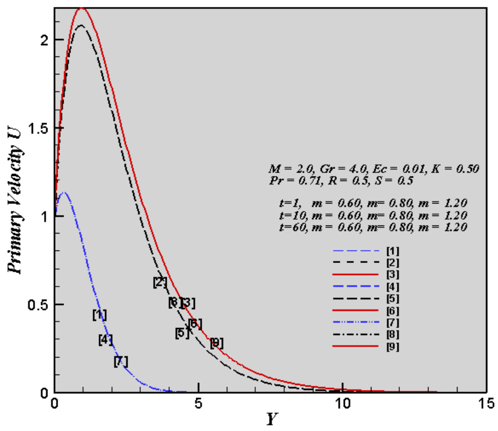

Figure- 3 Primary velocity profiles for the parameter m

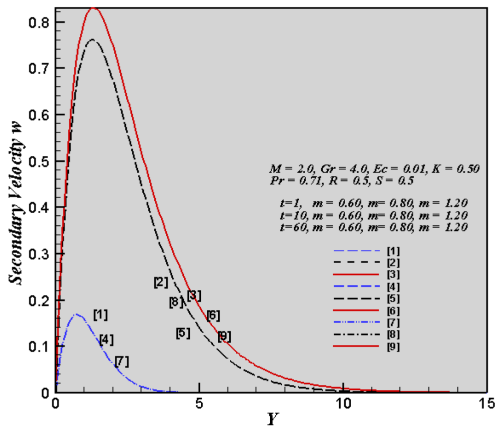

Figure- 4 Secondary velocity profiles for the parameter m

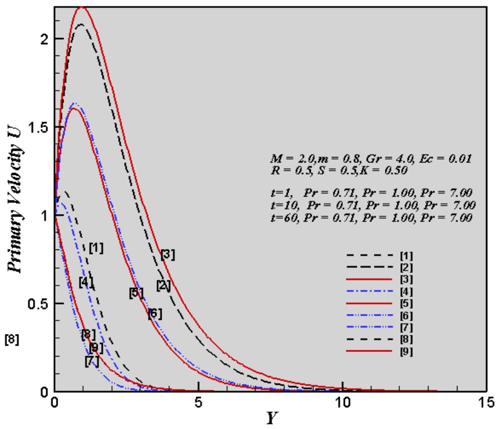

Figure- 5 Primary velocity profiles for the parameter P_r

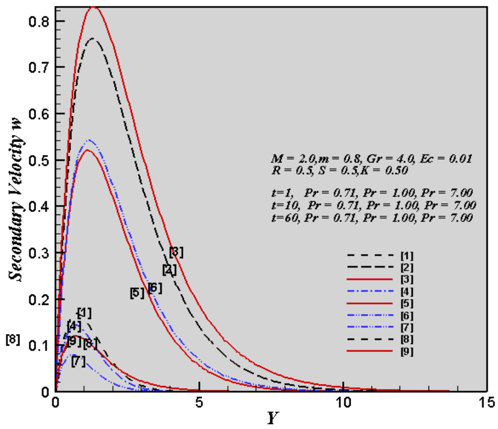

Figure- 6 Secondary velocity profiles for the parameter P_r

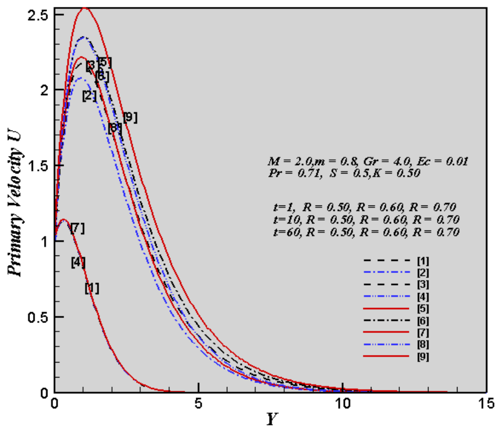

Figure- 7 Primary velocity profiles for the parameter R

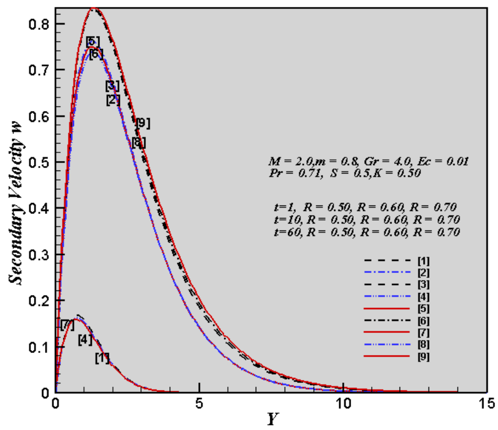

Figure- 8 Secondary velocity profiles for the parameter R

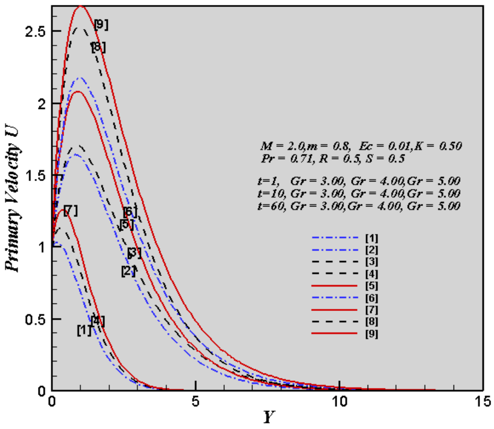

Figure- 9 Primary velocity profiles for the parameter G_r

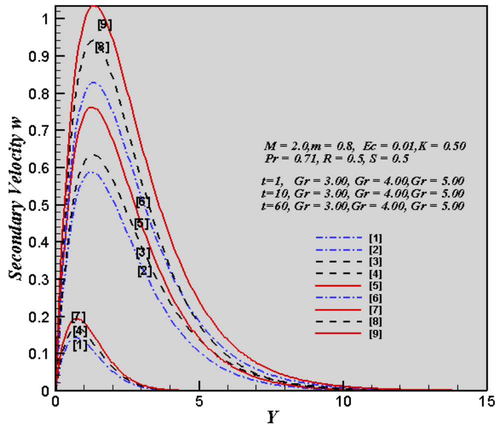

Figure- 10 Secondary velocity profiles for the parameter G_r

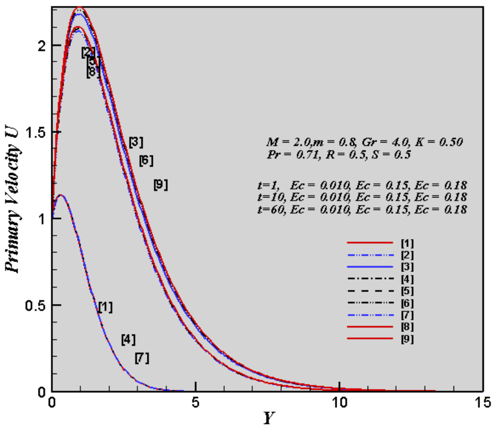

Figure- 11 Primary velocity profiles for the parameteE$_c$

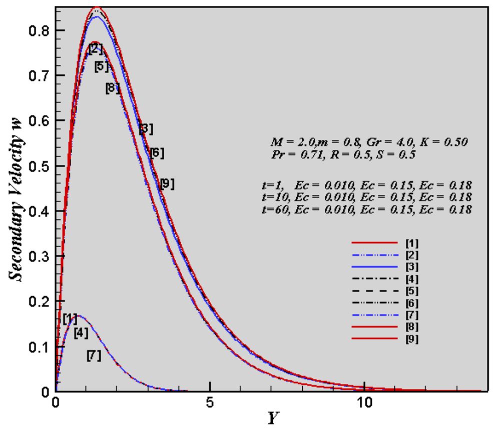

Figure- 12 Secondary velocity profiles for E_c

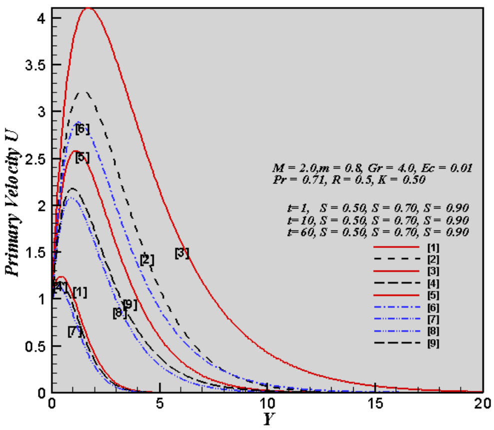

Figure- 13 Primary velocity profiles for the parameter S

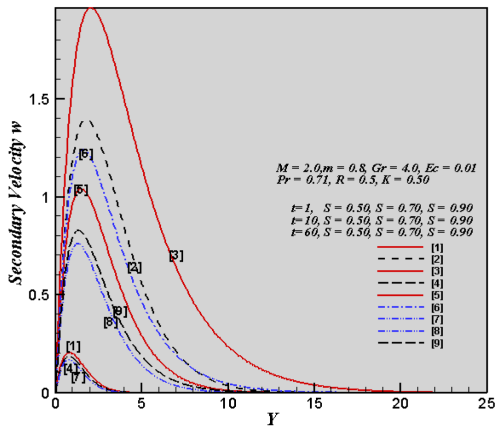

Figure- 14 Secondary velocity profiles for the parameter S

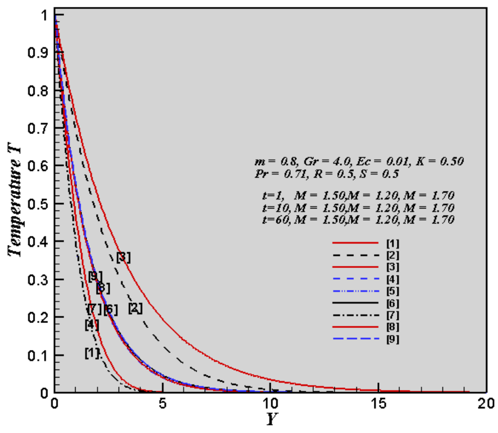

Figure- 15 Temperature profiles for the parameter *M*

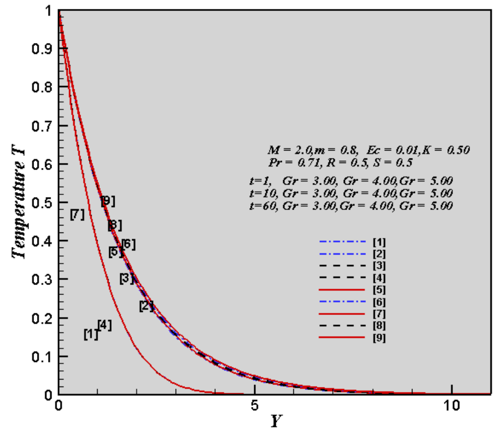

Figure- 16 Temperature profiles for the parameter G_r

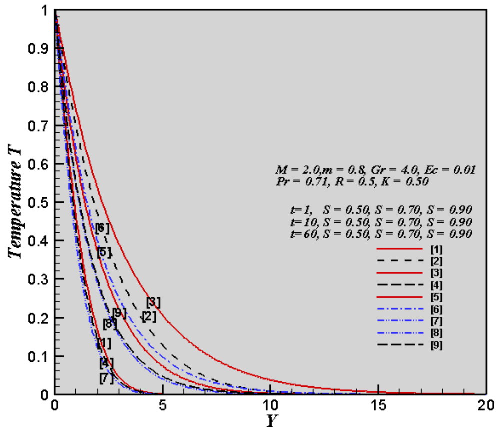

Figure- 17 Temperature profiles for the parameter *S*

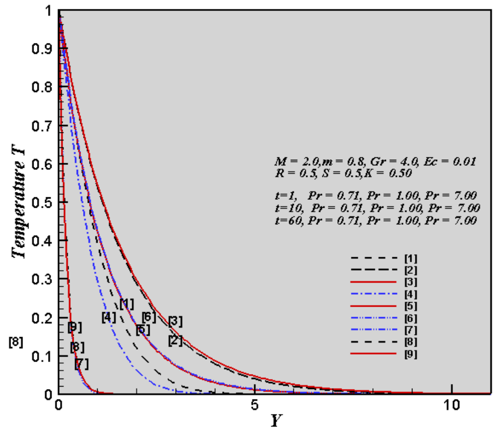

Figure- 18 Temperature profiles for the parameter P_r

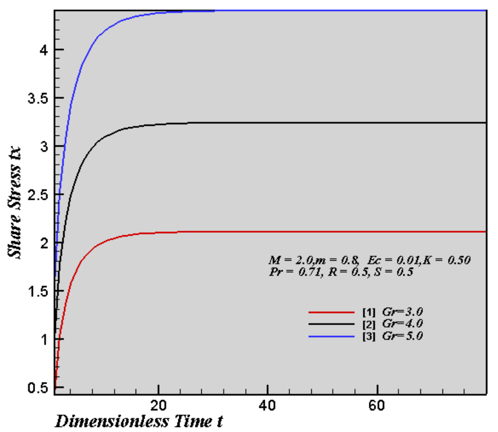

Figure- 19 Share Stress t_x for the parameter G_r

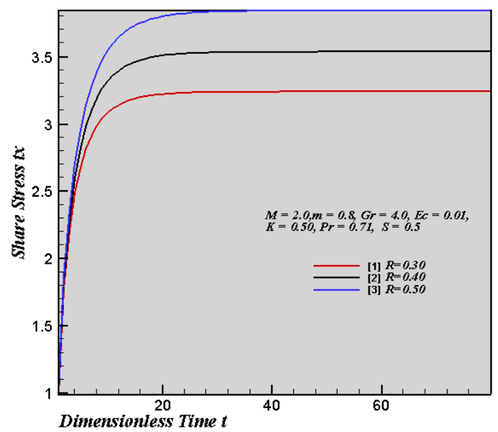

Figure- 20 Share Stress t_x for the parameter *R*

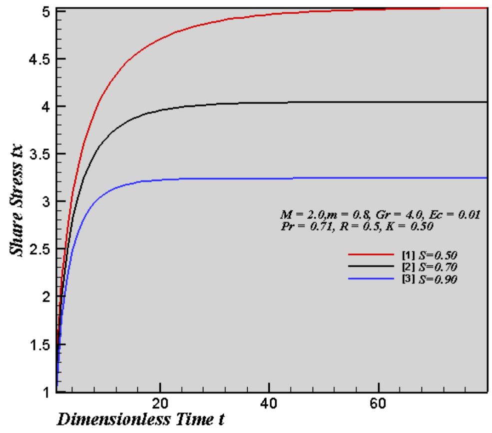

Figure- 21 Share Stress t_x for the parameter S

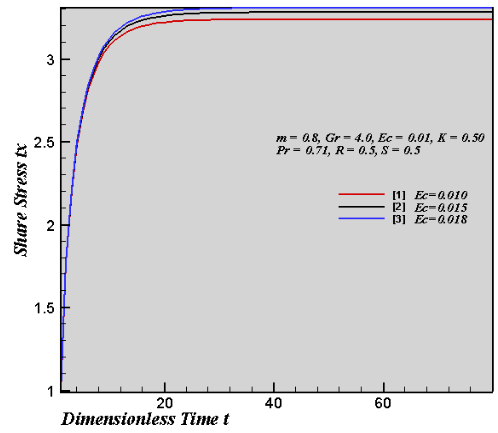

Figure-22 Share Stress t_x for the parameter E_c

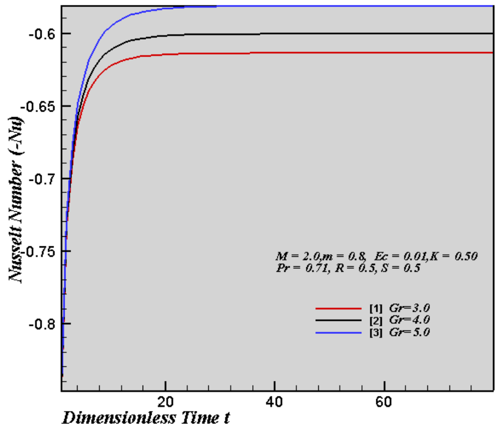

Figure- 23 Nusselt Number($-N_u$) for the parameter G_r

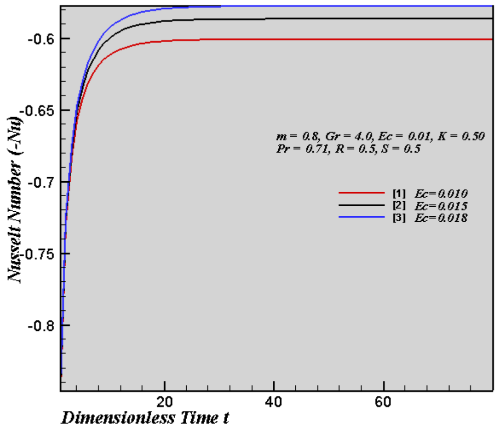

Figure- 24 Nusselt Number($-N_u$) for the parameter E_c

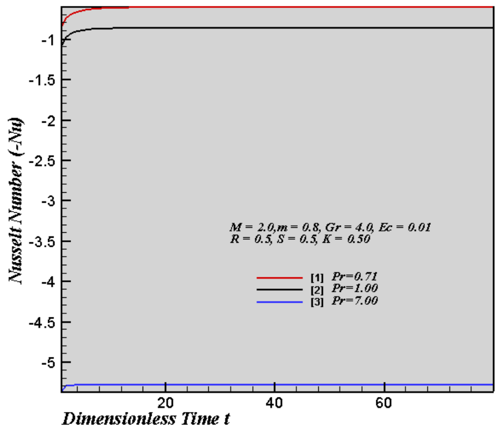

Figure- 25 Nusselt Number($-N_u$) for the parameter P_r

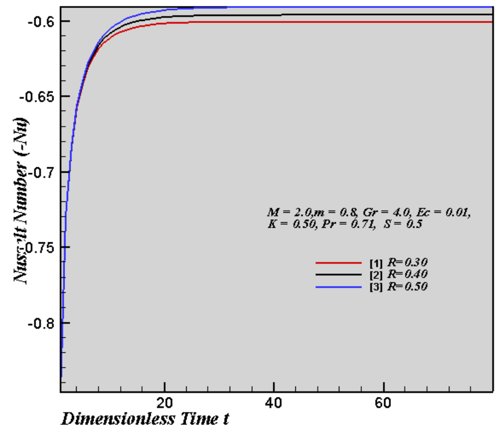

Figure- 26 Nusselt Number($-N_u$) for the parameter R

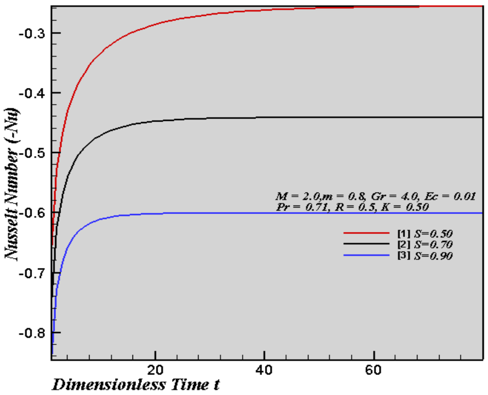

Figure- 27 Nusselt Number($-N_u$) for the parameter S

Qualitative comparison of the result with the previous result

Increased parameter	Previous result given by Anika and Nazmul					Present result				
	U	***W***	***T***	t_x	***-Nu***	***U***	***W***	***T***	t_x	***-Nu***
M	Dec	Inc	Dec	Dec	Inc	Dec	Dec	Dec	A bit impact	
P_r	Dec	Inc	Dec	Dec	Inc	Dec	Dec	Dec	A bit impact	Inc
R	Dec	Inc	Inc	Dec	Dec	Inc	Inc	A bit impact	Inc	Dec
G_r	Inc	Dec	Inc	Inc	Dec	Inc	Inc	Inc	Inc	Dec
E_c	Inc	Dec	Inc	Inc	Dec	Inc	Inc	A bit impact	Inc	Dec
S	Dec	Inc	Dec	Dec	Inc	Dec	Dec	Dec	Dec	Inc

Here, Dec= Decreasing, Inc= Increasing.

VI. CONCLUSIONS

In this study, the finite-difference solution on unsteady MHD fluid flow past a vertical porous plate has been considered in the presence of strong magnetic field, hall current m, rotating parameter R is investigated. In the present investigation, the Primary velocity, Secondary velocity increase with the increase of R, G_r, and E_c and decrease with the increase of M, P_r and suction S. The temperature distribution increases with the increase of G_r and decreases when M, P_r, and S are increase. The Nusselt-Number (-Nu) decreases with the increase of R, G_r, and E_c and increase when P_r and S are increase. The share stress t_x follow the trend of Primary velocity, Secondary velocity. The accuracy of present work is qualitatively good in case of all the flow parameters.

REFERENCES

[1] H. L. Agarwal, "P.C.Ram and V.Singh, Effects of Hall currents on the hydro-magnetic free convection with mass transfer in a rotating fluid." *Astrophysics and Space Science,* 100 (1984) 277-283.

[2] H. S. Takhar and P. C. Ram, "Effects of Hall current on hydro-magnetic free convection flow through a porous medium." *Astrophysics and Space Science*, 192(1992) 45-51.

[3] B. K. Sharma, A. K. Jha and R. C. Chaudhary, "Hall effect on MHD mixed convective flow of a viscous incompressible fluid past a vertical porous plate immersed in porous medium with heat source/sink." *Journal of Physics*, 52(5) (2007) 487-503.

[4] B. P. Garg, "Combined effects of thermal radiations and hall current on moving vertical porous plate in a rotating system with variable temperature." *International Journal of Pure and Applied Mathematics*, 81(2) (2012) 335-345.

[5] N. Islam and M. M. Alam, "Dufour and soret effects on steady MHD free convection and mass transfer fluid flow through a porous medium in a rotating system." *Journal of Naval Architecture and Marine Engineering,* 4 (2007) 43-55.

[6] Nisat Nowroz Anika, Md. Mainul Hoque and Nazmul Islam, Hall Current Effects on Magneto hydrodynamics Fluid over an Infinite Rotating Vertical Porous Plate Embedded in Unsteady Laminar Flow." *Annals of Pure and Applied Mathematics Vol. 3, No.2, 2013, 189-200.*

[7] S. F. Ahmmed, M. K. Das, L. E. Ali. Analytical Study on Unsteady MHD Free Convection and Mass Transfer Flow Past a Vertical Porous Plate. *American Journal of Applied Mathematics.* Vol. 3, No. 2, 2015, pp. 64-74. doi: 10.11648/j.ajam.20150302.16.

[8] E. M. Abo-Eldahaband, E. M. E. Elbarbary, "Hall current effect on magneto hydrodynamic free convection flow past a semi-infinite vertical plate with mass transfer." *Int. J. Engg.* Sci., 39 (2001) 1641-1652.

[9] M. A. Rana, A. M. Siddiqui and N. Ahmed, "Hall effect on Hartmann flow and heat transfer of a Burger's fluid." *Phys. Letters A,* 372 (2008) 562-568.